

## Longitudinal and transverse diffusion coefficients for $\text{Li}^+$ ion swarms in Kr gas

T. L. Tan, P. P. Ong, and M. M. Li

*Department of Physics, Faculty of Science, National University of Singapore, Lower Kent Ridge Road, Singapore 0511, Singapore*

(Received 23 March 1995)

The ratio of the transverse diffusion coefficient to mobility,  $D_T/K$  at 309 K for  $\text{Li}^+$  ion swarms drifting in Kr gas in the  $E/N$  (electric field to neutral gas number density ratio) range of 5 to 170 Td, was experimentally determined with an overall accuracy of  $\pm 4\%$ . The  $D_T/K$  results were effectively corrected for longitudinal end effects present appreciably in the drift tube by an analysis which requires the measurement of variance  $\langle x^2 \rangle$  of the transverse ion-current density profile at different drift lengths  $z$  and the derivation of the magnitude  $a_2$  of the end effects. Good agreement of the results with those calculated by Monte Carlo simulations (MCS) using an established interaction potential demonstrates the accuracy and reliability of the present  $D_T/K$  results. In addition, elaborate calculations of the reduced mobility  $K_0$  and ratio  $D_L/K$  of the longitudinal diffusion coefficient to mobility of the  $\text{Li}^+$ -Kr system are calculated with the MCS method. The accuracy of the MCS calculations is estimated to be  $\pm 2.5\%$ . The calculated  $D_L/K$  values are compared with the experimental data available in the literature. Both  $D_T/K$  and  $D_L/K$  values for  $\text{Li}^+$  in Kr were also derived using reduced mobility  $K_0$  data obtained from the MCS calculations and from experimental data, employing the generalized Einstein relations based on the three-temperature theory.

PACS number(s): 51.50.+v, 52.25.Fi, 34.20.Cf

### I. INTRODUCTION

There have been several experimental investigations of ion mobility [1–4] and longitudinal diffusion [3–5] of  $\text{Li}^+$  ions drifting in Kr gas in the last decade. However, so far, there is neither theoretical nor experimental reports on the transverse diffusion of the  $\text{Li}^+$ -Kr system. The importance of transverse diffusion which is usually expressed in terms of the ratio  $D_T/K$  of transverse diffusion coefficient to mobility is basically twofold. First, the measured values of  $D_T/K$  can be utilized to evaluate the accuracy of a proposed interaction potential by using the potential in a suitable model to calculate  $D_T/K$  values. If good agreement between the experimental and calculated values of  $D_T/K$  is found, then the proposed potential is considered to be a good representation of the true interaction potential. Second, in view of the small ion-neutral-atom mass ratio  $m/M$  of the  $\text{Li}^+$ -Kr system, the extent of the validity of the two-temperature (2T) kinetic theory [1] which favors small  $m/M$  can be further studied. Such investigation has been reported for the case of the  $\text{Li}^+$ -Xe system [6].

In this paper, we report our measurement of  $D_T/K$  values for a dilute swarm of  $\text{Li}^+$  ions drifting in Kr gas at values of electric field to neutral gas number density ratio,  $E/N$  ranging from 5 to 170 Td (1 Td =  $10^{-21}$  V m<sup>2</sup>) at  $309 \pm 1$  K. An effective correction technique to account for the presence of longitudinal end effects in the drift tube was employed to derive the final  $D_T/K$  values. These  $D_T/K$  values were compared with those calculated using the Monte Carlo simulation (MCS) technique which used the interaction potential due to Koutselos, Mason, and Viehland (KMV) [7] as input. The KMV po-

tential  $V(r)$  is shown in Fig. 1. To cover the wide range of  $V(r)$ ,  $V(r)$  axis is linear for  $V(r) < 0.02$  hartree and logarithmic for  $V(r) > 0.02$  hartree. In addition, the generalized Einstein relations (GER) were used to determine values of  $D_T/K$  using mobility  $K_0$  data obtained from the present MCS calculations and those reported [2–4]. Results of the calculations of  $D_L/K$  using the MCS technique are also reported and compared with those in the literature [4,5].

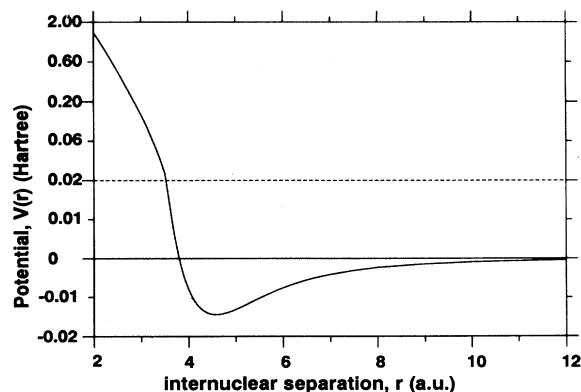


FIG. 1. The KMV potential  $V(r)$  as a function of internuclear distance  $r$ . The  $V(r)$ -axis scale is linear for  $V(r) < 0.02$  hartree and logarithmic for  $V(r) > 0.02$  hartree.

## II. EXPERIMENTAL METHOD

In the measurements, isotopically pure  ${}^7\text{Li}^+$  ions were produced by thermionic emission which is described in Ong, Hogan, and Tan [8]. The drift tube used in the present measurements has been used to measure  $D_T/K$  for  $\text{Na}^+$  ion swarms in several noble gases [9–12]. Essentially, the  $\text{Li}^+$  ions were released through a slit at one end of a variable-length drift tube and made numerous elastic collisions with spectrally but not isotopically pure Kr under the application of a uniform electric field  $E$  [13]. The gas was maintained at a constant pressure all the time. The transverse spatial profile of the ion-current density was recorded from the partial currents collected at each of the 33 gold-coated detecting rods which are positioned at the tail end of the drift tube. The variance  $\langle x^2 \rangle$  and the  $D_T/K$  value for a given  $E/N$  value and drift length  $z$  were then derived from the analysis [14] of the transverse ion-current profile recorded.

Systematic tests [14] showed that although the transverse diffusion data were independent of neutral gas pressure, conditions of ion injection into the drift tube, and ion space charge effects for the  $\text{Li}^+$ -Kr system, there was an appreciable dependence of the data on drift length. A total of four repeated measurements made at each of six different drift lengths ranging from 81.4 mm to 183.3 mm at  $E/N=35$  Td revealed that the  $D_T/K$  values were about 14% lower at the longest drift length as compared to those at the shortest drift length. For the case at  $E/N=140$  Td, the  $D_T/K$  values were 20% lower. These results confirmed that longitudinal end effects in the drift tube were extensively present for  $\text{Li}^+$  in Kr gas.

The transverse ion-current profiles for  $\text{Li}^+$ -Kr at the drift length  $z$  of 183.3 mm at  $E/N$  ranging from 5 to 170 Td were recorded at the constant pressure of 40.0 Pa at temperatures ranging from 308 to 310 K. At each  $E/N$  value, at least five ion-current profiles were recorded. The mean value of the variance  $\langle x^2 \rangle$  of each profile was determined using Eq. (4) given in Tan, Ong, and Hogan [15]. The minimum  $E/N$  value was limited by both the scarcity of the ion current under weak electric field and the ion-current profile spread which became too broad and extended into the radial boundary of the drift tube. The occurrence of electrical breakdown in Kr gas when the drift tube voltage exceeded 280 V restricted the upper limit of  $E/N$  to 170 Td.

## III. RESULTS AND DISCUSSION

A systematic and effective method for correcting longitudinal end effects to yield  $D_T/K$  results with accuracy comparable to that of a system without end effects is demonstrated in our experimental investigations on the  $\text{Na}^+$ -He system [15]. Using the same technique, the corrected  $D_T/K$  value and the value of  $a_2$  which quantifies the magnitude of end effects on the ion swarm have been derived for  $\text{Li}^+$  in Kr at  $E/N=35$  and 140 Td. Representative plots of  $\langle x^2 \rangle$  as a function of  $2z/E$  at  $E/N=35$  and 140 Td are shown in Figs. 2 and 3, respectively. The best-fit line in each figure is extrapolated

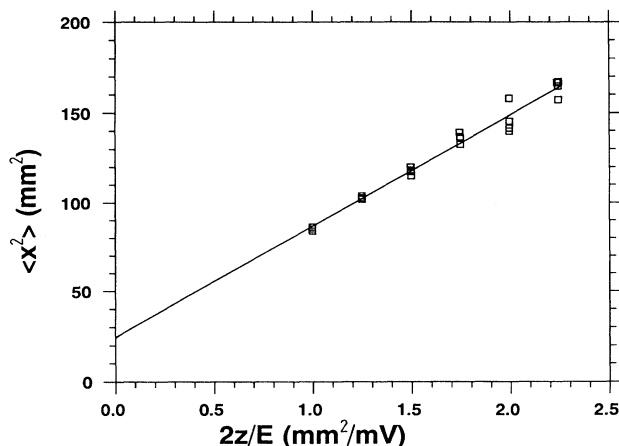


FIG. 2. The variance  $\langle x^2 \rangle$  plotted as a function of  $2z/E$  for  $\text{Li}^+$  ions in Kr at  $E/N=35$  Td. The solid line represents the best-fit line which is extrapolated to  $2z/E=0$  to find the value of  $a_2$  as given in Eq. (1).

to give the value of  $a_2$  at  $2z/E=0$  according to the equation

$$\langle x^2 \rangle = (D_T/K)(2z/E) + a_2. \quad (1)$$

Values of  $a_2$  which are given in Table I were found to be  $24.3 \pm 0.5$  and  $47.1 \pm 0.8$   $\text{mm}^2$  for  $E/N=35$  and 140 Td, respectively. While the  $a_2$  values are negative for  $\text{Na}^+$ -He [15] and  $\text{Rb}^+$ -He [16], they are positive for  $\text{Li}^+$ -Kr, suggesting that the direction of end effects is dependent on  $m/M$ . In addition, the  $D_T/K$  values which are derived from the gradient of the best-fit lines at  $E/N=35$

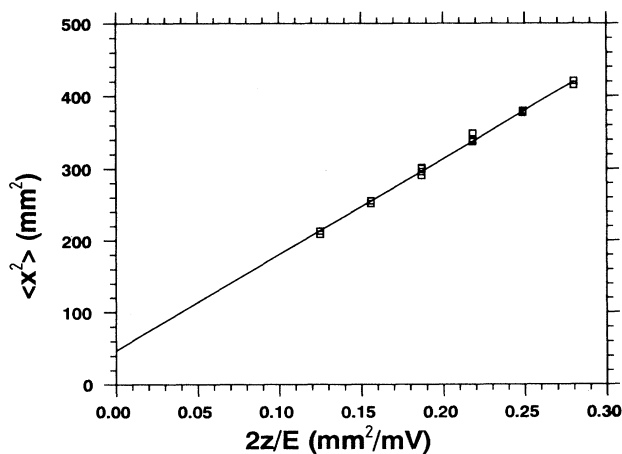


FIG. 3. The variance  $\langle x^2 \rangle$  plotted as a function of  $2z/E$  for  $\text{Li}^+$  ions in Kr at  $E/N=140$  Td. The solid line represents the best-fit line which is extrapolated to  $2z/E=0$  to find the value of  $a_2$  as given in Eq. (1).

and 140 Td are given in Table I. The two values of  $a_2$  at  $E/N=35$  and 140 Td were fitted with a straight line assuming a linear dependence of  $a_2$  on  $E/N$ . From this line, values of  $a_2$  at other  $E/N$  values were therefore obtained. Table I gives the values of  $a_2$  derived for  $\text{Li}^+$  in Kr at  $E/N$  ranging from 5 to 170 Td. Our previous experimental investigations which involved corrections for end effects in the  $\text{Na}^+\text{-Xe}$  [10],  $\text{Na}^+\text{-He}$  [15],  $\text{Rb}^+\text{-He}$  [16],  $\text{Rb}^+\text{-Ne}$  [17], and  $\text{Li}^+\text{-Xe}$  [18] systems have shown that  $a_2$  varies linearly with  $E/N$  for relatively low  $E/N$  (less than 200 Td). This observation allows us to confidently assume the linear dependence of  $a_2$  on  $E/N$  for the  $\text{Li}^+\text{-Kr}$  system. A set of  $a_2$  values can generally be linearly best-fitted with  $E/N$  with an overall accuracy of  $\pm 2\%$ .

Table I gives the measured values of  $\langle x^2 \rangle$ , together with the estimated standard deviations for  $\text{Li}^+\text{-Kr}$ . From the derived values of  $a_2$  and  $\langle x^2 \rangle$ , the value of  $D_T/K$  is finally calculated using Eq. (1). The  $D_T/K$  values given in Table I have been temperature corrected to 309 K using Eq. (1) given in Ref. [9]. The magnitude of the standard deviations of  $\langle x^2 \rangle$  given in Table I indicates that the random error in the values reported for  $\langle x^2 \rangle$  is less than  $\pm 2\%$ . However, the error in assuming the linear dependence of  $a_2$  on  $E/N$  and other minor er-

rors are expected to give an overall error for the experimental data of  $D_T/K$  to be within  $\pm 4\%$ .  $D_T/K$  values can be expressed more effectively [19] as reduced transverse diffusion coefficients  $D_T^{(r)}$  which are also given in Table I.

The MCS-calculated values of  $D_T^{(r)}$  for the  $\text{Li}^+\text{-Kr}$  system are provided in Table II. The results are expected to be better than 2.5%. Values of  $D_T^{(r)}$  calculated using the first and second generalized Einstein relations (GER) [1] from the mobility data of MCS calculations of Ellis *et al.* [3] and of Takebe *et al.* [4] are also given in Table II. Table III gives the reduced longitudinal diffusion coefficients  $D_L^{(r)}$  calculated using the MCS method and those derived from GER using the mobility values of the MCS calculations. The  $D_L^{(r)}$  values which are deduced from the experimental  $ND_L$  (product of longitudinal diffusion coefficient and neutral gas number density) and reduced mobility  $K_0$  of Ellis *et al.* [3] and of Takebe *et al.* [4] are also included in Table III for comparison.

As shown in Fig. 4, the reduced transverse diffusion coefficients  $D_T^{(r)}$  for  $\text{Li}^+\text{-Kr}$ , obtained from the present experimental results, and from the MCS calculations using KMV potential are in good agreement for  $E/N \leq 100$  Td. However, the experimental  $D_T^{(r)}$  results were consistently slightly higher (1–3%) than those from MCS calculations for  $E/N$  greater than 100 Td, indicating that the KMV repulsive potential is slightly on the softer side.

TABLE I. Experimental data of  $\langle x^2 \rangle$  with standard deviations (std. dev.),  $2z/E$ , and  $a_2$  for  $\text{Li}^+$  in Kr, and the derived values  $D_T/K$  and  $D_T^{(r)}$  (adjusted to 309 K).

$E/N$ (Td)	$\langle x^2 \rangle$ (mm <sup>2</sup> )	Std. dev. (mm <sup>2</sup> ) (%)		$2z/E$ (mm <sup>2</sup> /mV)	$a_2$ (mm <sup>2</sup> )	$D_T/K$ (mV)	$D_T^{(r)}$
5	228	2.1	0.9	7.82	17.8	27.0	0.990
10	132	1.4	1.1	3.91	18.9	29.0	0.994
15	104	1.6	1.6	2.61	20.0	32.1	0.994
20	92	0.9	1.0	1.95	21.0	36.3	0.988
25	89	0.9	1.0	1.56	22.1	42.6	1.004
30	90	1.5	1.7	1.30	23.2	51.0	1.034
35	95	1.2	1.3	1.12	24.3	62.8	1.092
40	102	1.0	1.0	0.98	25.4	78.2	1.166
45	111	1.0	0.9	0.87	26.5	97.8	1.258
50	124	1.7	1.4	0.78	27.6	124	1.381
55	141	1.8	1.3	0.71	28.6	158	1.530
60	161	1.2	0.8	0.65	29.7	202	1.715
65	183	0.9	0.5	0.60	30.8	253	1.896
70	203	1.7	0.8	0.56	31.9	306	2.035
75	221	2.8	1.2	0.52	33.0	361	2.139
80	239	1.6	0.7	0.49	34.1	418	2.222
85	258	1.5	0.6	0.46	35.2	483	2.313
90	277	1.9	0.7	0.43	36.2	554	2.398
95	295	1.7	0.6	0.41	37.3	626	2.461
100	310	0.6	0.2	0.39	38.4	693	2.485
110	340	2.0	0.6	0.36	40.6	842	2.536
120	369	1.3	0.3	0.33	42.8	1001	2.566
130	396	2.5	0.6	0.30	44.9	1168	2.577
140	419	2.0	0.5	0.28	47.1	1334	2.559
150	439	2.1	0.5	0.26	49.3	1492	2.510
160	456	3.3	0.7	0.24	51.4	1657	2.463
170	469	2.5	0.5	0.23	53.6	1805	2.388

TABLE II. MCS-derived values of  $D_T^{(r)}$  of  $\text{Li}^+$  in Kr using KMV potential and GER-derived values of  $D_T^{(r)}$  from the MCS calculations, Ellis *et al.* [3], and Takebe *et al.* [4].

$E/N$ (Td)	MCS $D_T^{(r)}$	Generalized Einstein relations (GER)		
		$D_T^{(r)}$ (MCS)	$D_T^{(r)}$ (Ellis <i>et al.</i> )	$D_T^{(r)}$ (Takebe <i>et al.</i> )
5	1.016	1.000		
10	1.005	1.002	0.973	0.989
15	0.996	1.005	0.978	0.993
20	0.996	1.011	0.985	1.002
25	1.014	1.015		1.003
30	1.042	1.016	1.000	1.010
35	1.089			1.023
40	1.168	1.068	1.061	1.060
45	1.275	1.127		1.125
50	1.375	1.201	1.203	1.208
55	1.529	1.306		1.317
60	1.714	1.403	1.479	1.456
65				1.608
70	2.054	1.705	1.802	1.771
80	2.189	1.960	2.014	2.027
90	2.388	2.147		2.220
100	2.459	2.305	2.365	2.380
110	2.510	2.414		
120	2.513	2.433	2.562	2.518
140	2.491	2.438		2.552
150			2.353	
160	2.401	2.331		2.534
180	2.256	2.255		2.419
200	2.164	2.162		
220				2.263

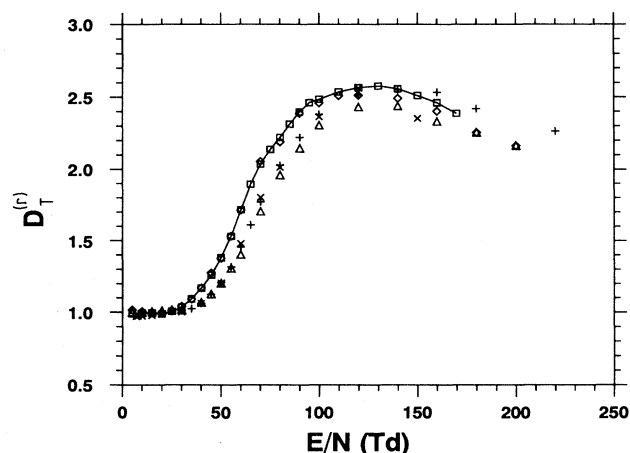


FIG. 4. Reduced transverse diffusion coefficients to mobility ratios  $D_T^{(r)}$  of  $\text{Li}^+$  in Kr plotted against  $E/N$ . Squares (connected by straight lines) and diamonds represent the present experimental data and MCS-calculated values using KMV potential, respectively. Triangles, crosses, and pluses represent GER-calculated values using mobilities from MCS calculations, from Ellis *et al.* [3], and from Takebe *et al.* [4], respectively.

This is evident from Fig. 1 in which the potential still remains finite even when the internuclear separation is reduced to zero. Similar behavior was also observed for the case of the  $\text{Li}^+$ -Xe system [18]. It can be seen from Fig. 4 that although the three sets of GER-calculated  $D_T^{(r)}$  data are in relatively good mutual agreement for  $E/N$  up

TABLE III. MCS- and GER-derived values of  $D_L^{(r)}$  of  $\text{Li}^+$  in Kr using KMV potential and experimental values of  $D_L^{(r)}$  from Ellis *et al.* [3] and Takebe *et al.* [4].

$E/N$ (Td)	MCS $D_L^{(r)}$	GER (MCS) $D_L^{(r)}$	Experimental data	
			$D_L^{(r)}$ (Ellis <i>et al.</i> )	$D_L^{(r)}$ (Takebe <i>et al.</i> )
5	0.994	1.006		1.980
10	1.008	1.025	1.070	1.862
15	1.000	1.054	1.154	1.717
20	1.051	1.089	1.211	1.535
25	1.078	1.136		1.419
30	1.139	1.181	1.380	1.281
35	1.388	1.314		1.573
40	1.586	1.440	2.007	2.046
45	1.948	1.715		2.182
50	2.246	1.961	2.820	2.517
55	2.597	2.199		3.346
60	3.010	2.543	3.850	3.690
65				3.798
70	3.410	3.068	4.168	3.962
80	3.343	3.123	4.308	4.029
90	3.223	3.157		3.807
100	3.015	3.172	4.210	3.541
110	2.867	2.888		
120	2.554	2.600	3.461	2.987
140	2.346	2.376		2.709
150			3.153	
160	2.105	2.093		2.330
180	1.963	2.026		2.065
200	1.771	1.939		2.014

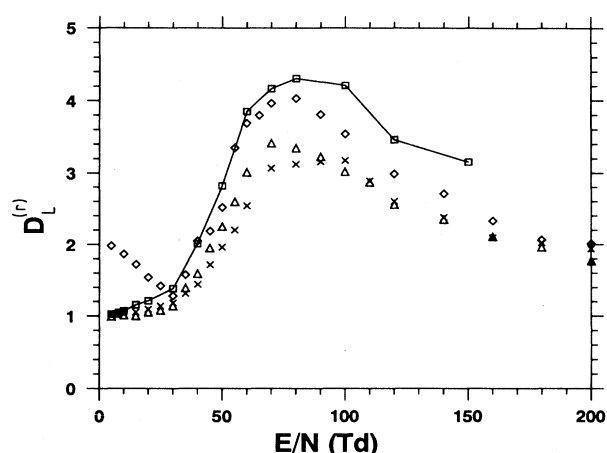


FIG. 5. Reduced longitudinal diffusion coefficient to mobility ratios  $D_L^{(r)}$  of  $\text{Li}^+$  in Kr plotted against  $E/N$ . Squares (connected by straight lines) and diamonds represent the experimental data of Ellis *et al.* [3] and of Takebe *et al.* [4], respectively. Triangles and crosses represent MCS-calculated values using KMV potential and GER-calculated values using mobilities from MCS calculations, respectively.

to 150 Td, they were up to 16% lower than those from the present experiments and from MCS calculations for  $E/N$  values from 30 to 150 Td. This can be explained from the fact that GER calculations using the three-temperature (3T) theory are not expected to be accurate when the ion-neutral-atom mass ratio is not negligible and in the  $E/N$  region where the mobility rises rapidly [1].

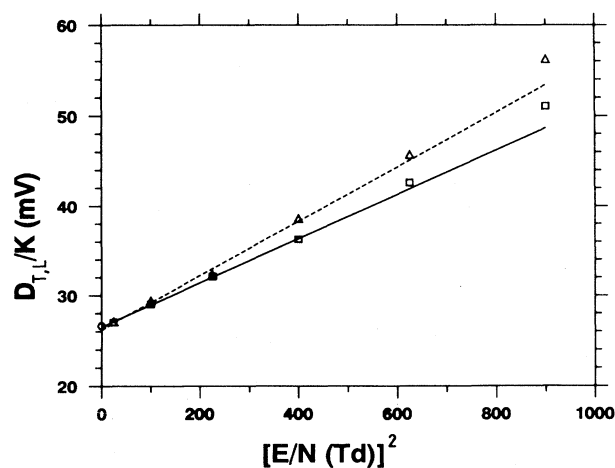


FIG. 6. Plots against  $(E/N)^2$  of  $D_T/K$  for the present experimental data points (squares) and of  $D_L/K$  for the MCS (KMV) data points (triangles) showing their y intercepts for  $\text{Li}^+$  in Kr. The theoretical limit value of 26.6 mV at 309 K is shown as a single hexagon on the y axis. The continuous and broken lines represent, respectively, the best-fit straight lines to the  $D_T/K$  and  $D_L/K$  data points for  $E/N \leq 20$  Td.

A comparison of the various  $D_L^{(r)}$  data is displayed in Fig. 5. The directly calculated MCS data for  $D_L^{(r)}$  agree fairly well with those calculated from MCS mobility data using the GER relations throughout the whole  $E/N$  range (5–200 Td). However the  $D_L^{(r)}$  values derived from the experimental data of Ellis *et al.* [3] and of Takebe *et al.* [4] were found to be up to 32% and 25%, respectively, higher than the MCS-derived data at values of  $E/N$  around the peak region and higher. The large discrepancy of the data of Ellis *et al.* [3] is probably caused by a systematic error in the measurements made with the Georgia Tech drift-tube mass spectrometer [9,14]. At  $E/N$  below 30 Td, the  $D_L^{(r)}$  values of Takebe *et al.* [4] were found to be unrealistically higher than the rest of the data, as shown in Fig. 5. The higher  $D_L^{(r)}$  values as compared to those from MCS calculations throughout the whole  $E/N$  range could be the result of some end effects which were not totally eliminated in their drift tube of maximum drift distance of 6.0 cm [4]. In a similar trend, the investigation of Takebe *et al.* [4] shows that their measured  $ND_L$  values were largely higher than those from their calculations using GER. The same result was also found by Thackston *et al.* [5] in their  $ND_L$  measurements for  $\text{Li}^+\text{-Kr}$ .

The accuracy of the present experimental  $D_T/K$  results and of the  $D_L/K$  values calculated using MCS can be demonstrated from a plot of  $D_T/K$  and  $D_L/K$  with  $(E/N)^2$  at very low  $E/N$ . As  $E/N$  tends to zero,  $D_T/K$  and  $D_L/K$  should vary linearly and approach the theoretical limit of 26.6 mV for  $T=309$  K as  $E/N \rightarrow 0$  as predicted by the Einstein equation, given in Ref. [9].

This behavior as shown in Fig. 6 indicates the accuracy of the present experimental  $D_T/K$  and MCS-calculated  $D_L/K$  using the KMV potential.

#### IV. CONCLUSION

This paper presents our experimental data of  $D_T/K$  for the heretofore unstudied system of  $\text{Li}^+$  ions in Kr with an overall accuracy of 4% in the range  $E/N=5$  to 170 Td. They are effectively corrected for longitudinal end effects present in the drift tube. These  $D_T/K$  data are useful as input values for the determination of ion-neutral interaction potential particularly in the medium and long-range regions, and with which theoretical calculations can be compared. Experimental values of  $D_T/K$  were found to be in good agreement with the calculations of the MCS method based on the KMV potential, particularly at  $E/N \leq 100$  Td. This shows the validity of the KMV potential curve for the  $\text{Li}^+\text{-Kr}$  system in this  $E/N$  range. The MCS-calculated  $D_L/K$  values were up to about 30% lower than those experimental values reported in the literature.

#### ACKNOWLEDGMENTS

We are grateful to Mr. Wu Tong Meng for his efficient technical assistance during the course of the experiments. This work was supported by National University of Singapore Grant No. RP910651. We thank the staff of the University's Computer Center for the use of the supercomputer system.

- 
- [1] E. A. Mason and E. W. McDaniel, *Transport Properties of Ions in Gases* (Wiley, New York, 1988).
  - [2] M. S. Byers, M. G. Thackston, R. D. Chelf, F. B. Holleman, J. R. Twist, G. W. Neeley, and E. W. McDaniel, *J. Chem. Phys.* **78**, 2796 (1983).
  - [3] H. W. Ellis, M. G. Thackston, E. W. McDaniel, and E. A. Mason, *At. Data Nucl. Data Tables* **31**, 113 (1984).
  - [4] M. Takebe, Y. Satoh, K. Iinuma, and K. Seto, *J. Chem. Phys.* **76**, 2672 (1982).
  - [5] M. G. Thackston, M. S. Byers, F. B. Holleman, R. D. Chelf, J. R. Twist, and E. W. McDaniel, *J. Chem. Phys.* **78**, 4781 (1983).
  - [6] P. P. Ong, *Phys. Rev. E* **47**, 4323 (1993).
  - [7] A. D. Koutselos, E. A. Mason, and L. A. Viehland, *J. Chem. Phys.* **93**, 7125 (1990).
  - [8] P. P. Ong, M. J. Hogan, and T. L. Tan, *Phys. Rev. A* **46**, 5706 (1992).
  - [9] T. L. Tan, P. P. Ong, and M. J. Hogan, *Phys. Rev. E* **48**, 1331 (1993).
  - [10] T. L. Tan, P. P. Ong, and M. J. Hogan, *J. Chem. Phys.* **100**, 586 (1994).
  - [11] P. P. Ong, T. L. Tan, and K. Y. Lam, *J. Phys. B* **26**, 2649 (1993).
  - [12] T. L. Tan and P. P. Ong, *J. Phys. B* **27**, 1525 (1994).
  - [13] P. P. Ong and M. J. Hogan, *Rev. Sci. Instrum.* **62**, 1047 (1991).
  - [14] M. J. Hogan and P. P. Ong, *J. Phys. D* **23**, 1050 (1990).
  - [15] T. L. Tan, P. P. Ong, and M. J. Hogan, *J. Phys. D* **27**, 84 (1994).
  - [16] P. P. Ong and T. L. Tan, *J. Chem. Phys.* **102**, 963 (1995).
  - [17] T. L. Tan and P. P. Ong (unpublished).
  - [18] T. L. Tan and P. P. Ong, *J. Phys. B* (to be published).
  - [19] P. P. Ong, M. J. Hogan, K. Y. Lam, and L. A. Viehland, *Phys. Rev. A* **45**, 3997 (1992).